Supporting Information for:

In situ probe of photocarrier dynamics in water-splitting hematite (α-Fe_2O_3) electrodes

Zhuangqun Huang,[a] Yongjing Lin,[b] Xu Xiang,[c] William Rodríguez-Córdoba,[a] Kenneth J. McDonald,[d] Karl S. Hagen,[a] Kyoung-Shin Choi,[d] Bruce S. Brunschwig,[e] Djamaladdin G. Musaev,[f] Craig L. Hill,[a] Dunwei Wang,[b] and Tianquan Lian*[a]

[a] *Department of Chemistry, Emory University, Atlanta, Georgia 30322, United States; Fax: 404 727 6586; Tel: 404 727 6649; Email: tlian@emory.edu*
[b]*Department of Chemistry, Merkert Chemistry Center, 2609 Beacon Street, Boston College, Chestnut Hill, Massachusetts 02467, United States*
[c] *State Key Laboratory of Chemical Resource Engineering, Beijing University of Chemical Technology, Beijing 100029, PR China* [d]*Department of Chemistry, Purdue University, West Lafayette, Indiana 47907, United States*
[e] *Beckman Institute, California Institute of Technology, Pasadena, California, 91125, United States*
[f] *Cherry L. Emerson Center for Scientific Computation, Emory University, Atlanta, Georgia 30322, United States*

***Corresponding Authors:** tlian@emory.edu

Table of Contents:

1. Materials

All the chemicals and solvents were purchased commercially and used without further purification.

2. Instrumentation

FTIR, UV-Vis, potentiostat and Stark spectrometer. The FTIR spectra were measured on a Thermo Nicolet 6700 spectrometer. UV-Vis spectra were acquired using Agilent 8453 spectrophotometer equipped with a diode-array detector and an Agilent 89090A cell temperature controller unit. The electrochemical work station is a BAS CV-50W voltammetric analyzer (BASi).

The Stark apparatus, experimental methods and data collection procedure were previously reported.[1] Briefly, the white light generated from a 15 V/150 W halogen lamp was focused on the entrance slit of a Spex 270 M monochromator via a spherical concave mirror (focal length 600 mm, diameter 5.0 cm) and a plane mirror (diameter 2.5 cm). The dispersed light exiting the monochromator was depolarized (DPL, diameter 2.5 cm, CVI), horizontally polarized (calcite polarizer, CVI), and then focused onto the sample cell inside the Dewar with a convex quartz lens (focal length 190 mm, diameter 5.0 cm). The applied electric field was generated by a Rolfe high-voltage power supply which produces an ac peak-to-peak voltage of 0−10 kV at 100−600 Hz. After the sample, the transmitted light was refocused onto the UV-enhanced silicon diode (UDT-555UV, 500 or 50 kΩ feedback resistor) via a convex lens (focal length 190 mm, diameter 5.0 cm). Two strips of Kapton film (50 μm, Dupont) were arranged so that they lay flush with the two long edges of the sample and a counter FTO glass.

3. Synthesis

Atomic Layer Deposition of hematite thin films followed our established procedures.[2] Electrochemical deposition of nanoparticle films has been reported reviously.[3,4] Colloidal hematite particles in aqueous solution were synthesized by forced electrolysis following the procedures by Tokunaga et. al.[5]

4. Transient Spectroscopic Studies

(a) Ultrafast Visible Transient Absorption Measurements. Our femtosecond transient absorption spectrometer is based on a regeneratively amplified Ti:sapphire laser system (coherent Legend, 800 nm, 150 fs, 3 mJ/pulse and 1 kHz repetition rate) and the Helios spectrometer (Ultrafast Systems LLC). The excitation pulse at 400 nm was generated by doubling the frequency of the fundamental 800 nm pulse in a β-barium borate (BBO) type I crystal. The

energy of the 400 nm pump pulse was controlled to be ~100 nJ/pulse with a neutral density filter. The pump beam diameter at the sample was ~400 μm. A white light continuum (WLC) (450~720 nm), used as a probe, was generated by attenuating and focusing 10 μJ of the fundamental 800 nm pulse into a sapphire window. This WLC was split in two parts used as a probe and reference beams. The probe beam was focused with an aluminum parabolic reflector into the sample with a beam diameter of ~150 μm. The reference and probe beams were focused into a fiber-coupled multichannel spectrometer with CMOS sensors and detected at a frequency of 1 kHz. To minimize low-frequency laser fluctuations every other pump pulse was blocked with a synchronized chopper (New Focus Model 3501) at 500 Hz, and the absorbance change was calculated with two adjacent probe pulses (pump-blocked and pump-unblocked). The delay between the pump and probe pulses was controlled by a motorized translational stage. In all transient absorption spectra, the chirp and time zero correction were performed with Surface Explorer software (v.1.1.5, Ultrafast Systems LCC) using a dispersion correction curve obtained by fitting the representative kinetics of the transient absorption experiments of the solvent. The typical instrument response of our spectrometer is well represented by a Gaussian function with a full width at half-maximum (FWHM) of 180 ± 10 fs.

(b) Ultrafast Visible Pump/IR Probe Transient Absorption Measurements. Our tunable femtosecond infrared spectrometer is based on a Clark IR optical parametric amplifier (OPA) which generates two tunable near-IR pulses in the 1.1 to 2.5 μm spectral range (signal and idler, respectively). The broad mid-IR pulses centered at 2000 cm^{-1} were generated by difference frequency generation (DFG) combining the corresponding signal and idler in a 1-mm-thick type II $AgGaS_2$ crystal. The frequency tuning of the mid-IR pulses was achieved by changing the signal and idler frequencies at the OPA and optimizing the timing between the pulses and the phase matching angles of the BBO (OPA crystal) and the $AgGaS_2$ crystal. After the difference frequency generation, the mid-IR pulse was collimated and split in two parts with a 90% beamsplitter. The 10% transmitted part was used as a probe in the Visible-IR transient absorption measurements**.** To prevent cumulative heating in the sample and to avoid the saturation of the detector, the intensity of the probe mid-IR pulse was attenuated using neutral density filters to approximately 40 μJ, before it was focused into a 0.4 μm CaF_2 path-length cell containing the sample. At the focal point, the probe was spatially overlapped with the temporally delayed 400 nm excitation pulse with pump energy of about 2 μJ/pulse, respectively. The diameter of the pump and probe beams were 400 and 200 μm, respectively. The mid-infrared probe pulse was spectrally dispersed with an imaging spectrograph (CVI, Digikrom 240) and imaged onto a 32-element infrared HgCdTe (MCT) array detector. The difference absorption spectra were

calculated by subtracting the absorption spectrum of the excited sample from the absorption spectrum of the sample in the ground state by blocking every other pump pulse with a phase-locked optical chopper (New Focus) at 500 Hz. The instrument response function of our spectrometer was well represented by a Gaussian function with a 230 ± 10 fs full width at half-maximum (FWHM), respectively.

(c) **Nanosecond transient absorption measurements**

Measurements at the ns to μs scales were carried out in an EOS spectrometer (Ultrafast Systems LLC). The pump pulses at 400 nm were generated from the same laser system described above. The probe pulse, a 0.5-ns white-light source operating at 20 kHz, was synchronized with the femtosecond amplifier, and the delay time was controlled by a digital delay generator. The probe light was detected in a fiber-optic-coupled multichannel spectrometer with a complementary metal−oxide−semiconductor (CMOS) sensor. The absorbance change was calculated from the intensities of sequential probe pulses with and without the pump.

5. Transient Spectra of Different Hematite Films

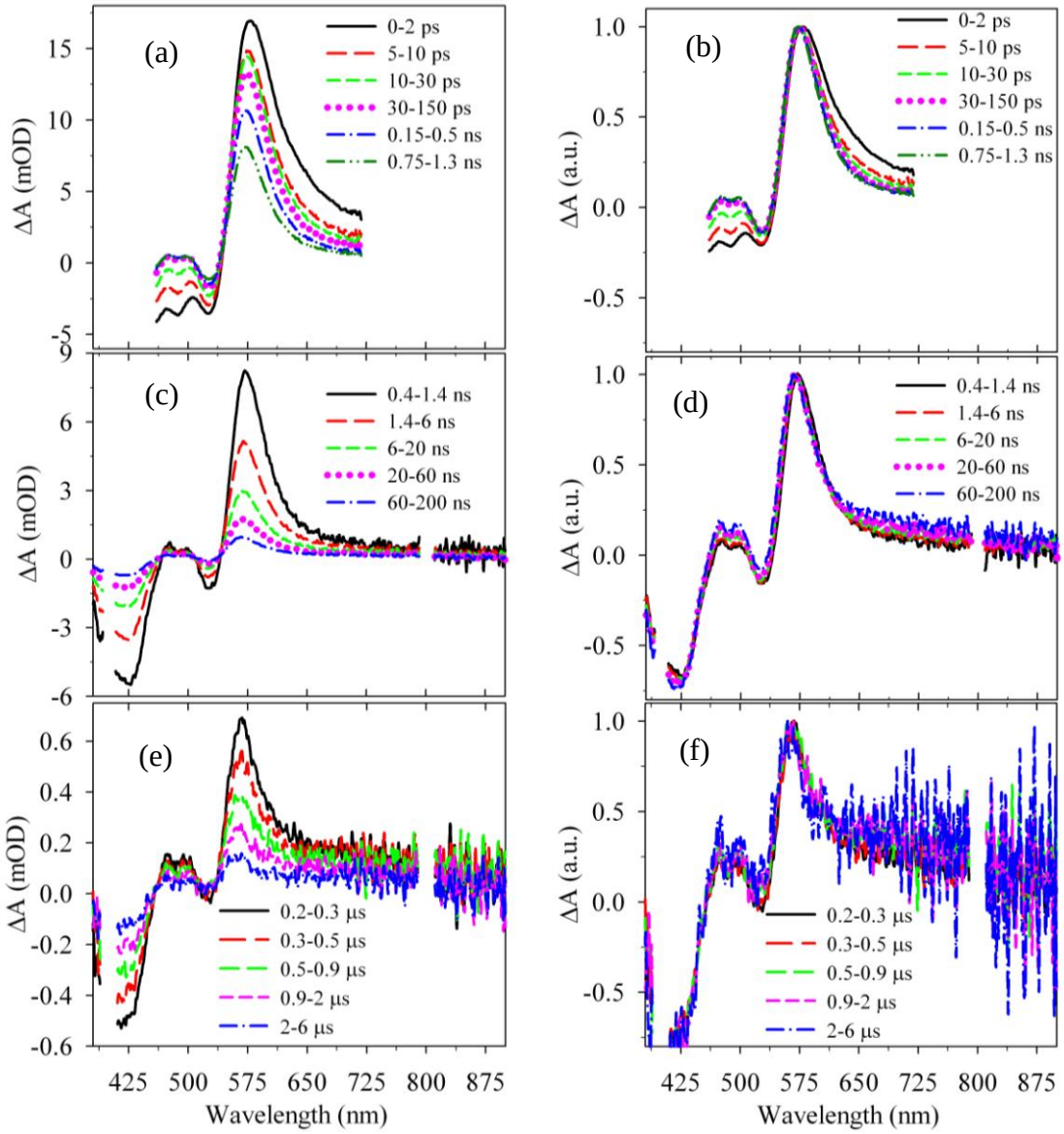

Figure S1. Averaged TA spectra of hematite thin film (30 nm, grown by atomic layer deposition) after 400 nm excitation: (a) 0-1.3 ns, measured in femtosecond TA set up with a probe white light from 470 to 720 nm; (b) Normalized comparison of spectra shown in (a); (c) 0.4-200 ns, measured in the nanosecond TA set up with a probe white light from 380 to 900 nm; and (d) Normalized comparison of the spectra shown in (c). (e) 0.2-6 μs, measured in the nanosecond TA set up; and (f) Normalized comparison of the spectra shown in (e). Spectral data at ~ 400 nm and ~800 nm in the ns spectra are not available due to the interference of the pump beam.

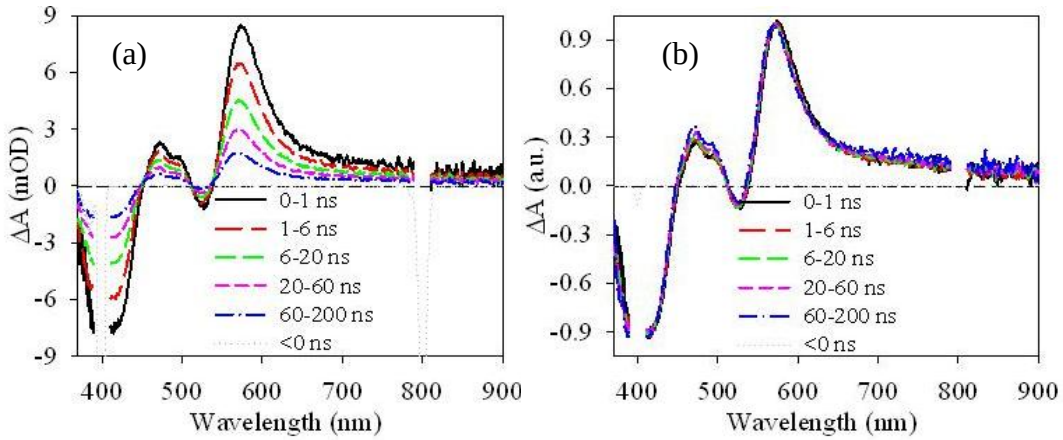

Figure S2. (a) Averaged TA spectra of hematite thin film (42 nm, grown by atomic layer deposition) after 400 nm excitation. (b) Normalized comparison of spectra shown in (a). Spectral data at ~400 nm and ~800 nm in the ns spectra are not available due to the interference of the pump beam.

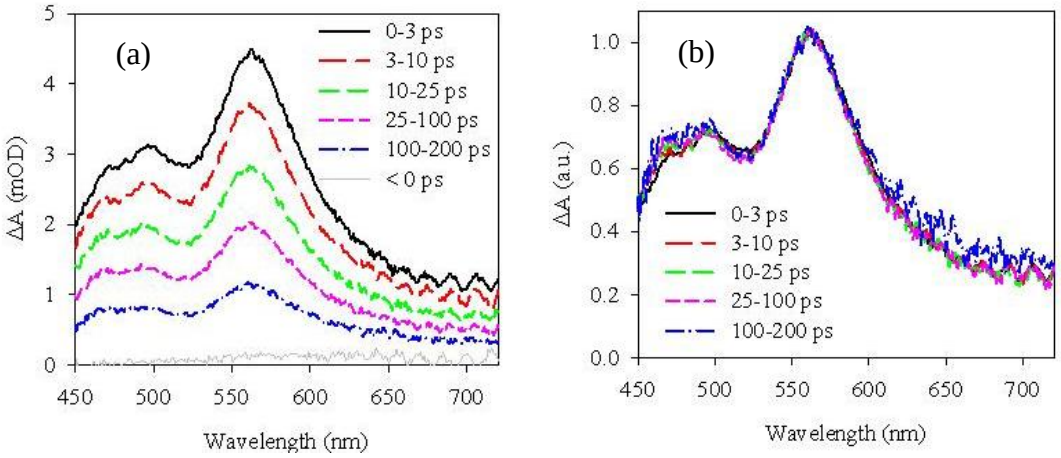

Figure S3. (a) Averaged transient absorption spectra of hematite colloidal particles (synthesized by forced hydrolysis[5]) at indicated delay time windows after 400 nm excitation; (b) Normalized comparison of TA spectra shown in (a).

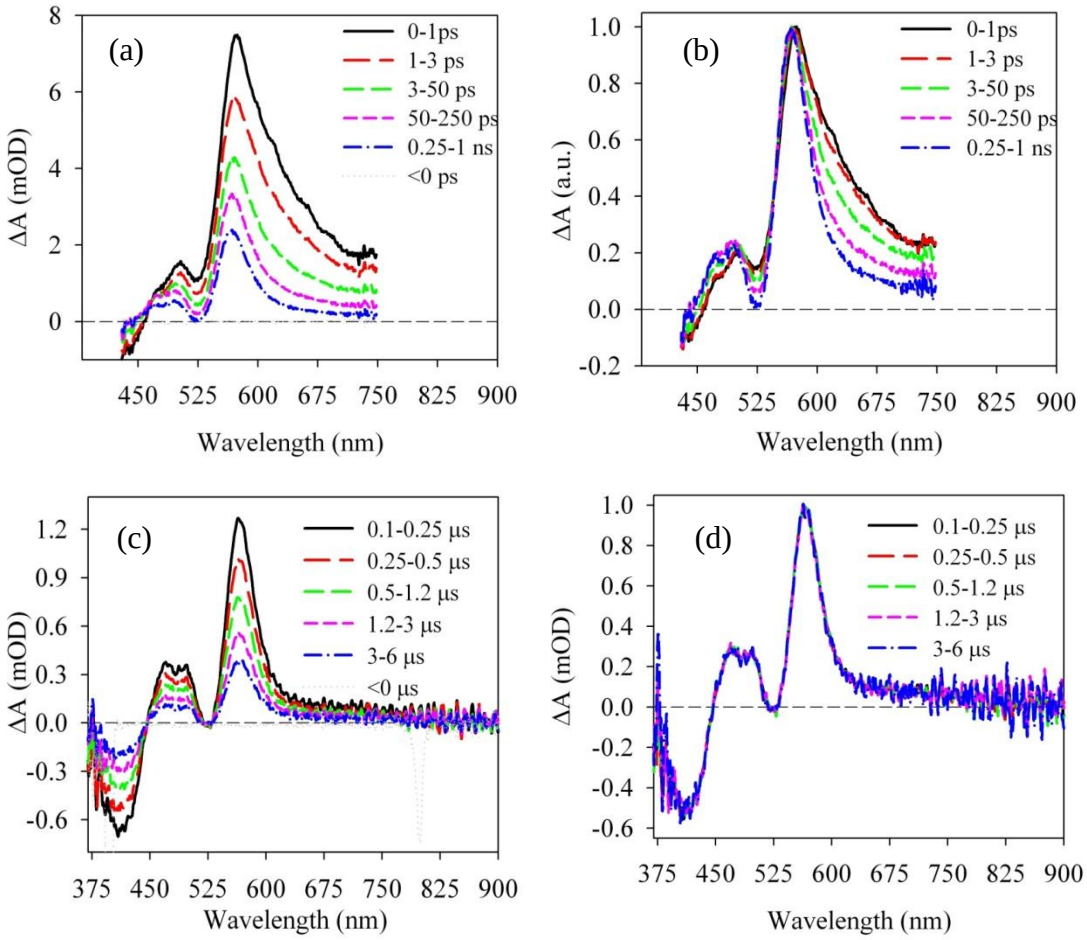

Figure S4. Averaged TA spectra of hematite nanoparticle thin films (30 nm, prepared by electrochemical deposition[3,4]) at indicated delay time windows after 400 nm excitation: (a) 0-1 ns, measured by the femtosecond TA set up with a probe white light from 440 to 750 nm; (b) Normalized comparison of TA spectra shown in (a); (c) 0.1-200 ns, measured by the nanosecond TA set up with a probe white light from 380 to 900 nm; and (d) Normalized comparison of TA spectra shown in (c).

6. Bias Dependent Differential UV-Vis Spectra

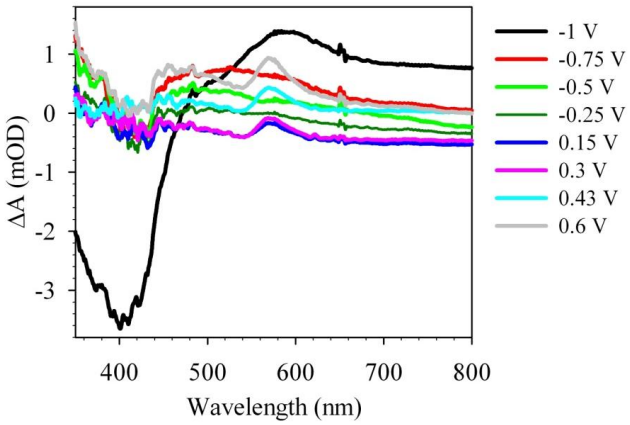

Figure S5. Differential UV-Vis spectra of hematite films at indicated external biases. These spectra were generated by subtracting off the spectrum *at* open circuit. Conditions: reference electrode, Ag/AgCl (3 M NaCl); counter electrode, Pt wire; electrolyte, 1 M NaOH. Each spectrum is an average of 20 spectra taken under the same conditions.

7. Estimate of the Maximum Transient Electric Field

The maximum electric field after 1 ns can be estimated using a model of parallel-plate capacitor, where all the photo-generated charges line up in an ideal manner: with the opposite charges at two sides of the film. This simplified and idealized parallel-plate model is a reasonable approximation because compared to the thickness of the film (30 nm), the beam size can be treated as infinite (400 μm). The photogenerated electric dipoles in reality would be much more disordered and the light-induced built-in electric field would be smaller than the value estimated here.

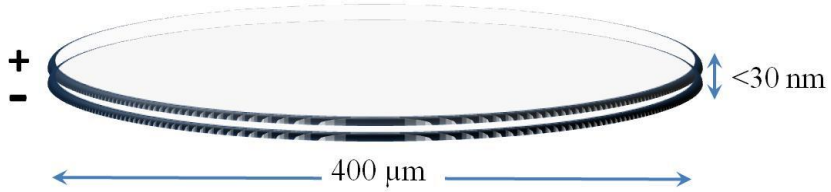

Figure S6. Schematic presentation of the parallel-plate capacitor model.

Typical parameters:

- Photon energy per pulse: E_{ph} = 100 nJ
- Wavelength: λ = 400 nm, or frequency: $\nu = 7.5 \times 10^{14}$ Hz

- Absorption at 400 nm: $A = 0.6$
- Beam size: $d = 400\ \mu m$
- Hematite static dielectric constant: $\varepsilon = 60$. Dielectric constant values quoted in literatures vary widely from 30 to 120. We used 60 here for the consistency with our previous report. [2,6]
- Hematite refractive index at 400 nm: $n = 2.1$[7] Other studies reported larger n values up to 3.0. Here we used 2.1 as a conservative estimation.

(a) Number of incident photons, N:

$$N = \frac{E_{ph}}{h\nu} = 2 \times 10^{11}$$

h is Planck constant; and c is the speed of light

(b) Charge density, if all photons are absorbed and the quantum yield of charge separation is 1:

$$\sigma = \frac{Ne}{\pi\left(d/2\right)^2} = 0.26\, C \cdot m^{-2}$$

where e is the elementary charge (1.6×10^{-19} C)

(c) Maximum electric field:

$$E = \frac{\sigma}{\varepsilon_0 \varepsilon} = 4.8 \times 10^8 V/m$$

where ε_0 is vacuum permittivity.

Several corrections need to be made:

i) The absorbance at 400 nm is 0.6, resulting in a correction factor for σ of $(1\text{-}10^{-A}) = 0.75$ due to the transmission loss.

ii) If a normal incident is assumed, we have the second correction factor of $1\text{-}(2.1\text{-}1)^2 / (2.1 + 1)^2 = 0.65$ (Fresnel equation) due to the reflection loss.

iii) In this paper, we mainly focus on assignment of the transient spectra after 1 ns (Figure 4). At 1 ns, > 80% electron-hole pairs have recombined (Figure 3). Assuming the transient signal is linearly proportional to the charge density, a correction factor of (1 - 0.8) = 0.2 can be applied.

Then, we have a corrected charge density:

$$\sigma_{corrected} = 0.75 \times 0.65 \times 0.2 \times \sigma = 0.10 \times \sigma$$

yielding of an estimated field of:

$$E_{corrected} = 4.8 \times 10^7 V/m$$

It should be noted that, first, in our experiment, the pump is off normal incident direction, resulting in higher reflection loss. In addition, in reality, the photogenerated electric dipoles could be randomly distributed among the whole sample. The consequence of all these factors will result in a much smaller build-in transient electric field.

In our Stark measurement, we applied an electric field of 2 x 10^7 V/m (1000 V, 50 μm spacer) to the ALD hematite sample using another FTO slide as a counter electrode to build a parallel-plate capacitor. A voltage higher than 1000 V will result in a dielectric breakdown. This field strength (2 x 10^7 V/m) is similar to the estimated maximum electric field (4.8 x 10^7 V/m) in the model described above and could be much larger than the real transient electric field in the sample. However, under this electric field, we only observed Stark signals < 0.2 mOD (data are not shown here), which is over 50 times smaller than the transient signals at 1 ns (~10 mOD). Therefore, the transient Stark signal (even if it exists) in our experiment contributes very little to the transient signal.

8. Photoelectrochemical Performance of the Electrode under Laser Illumination

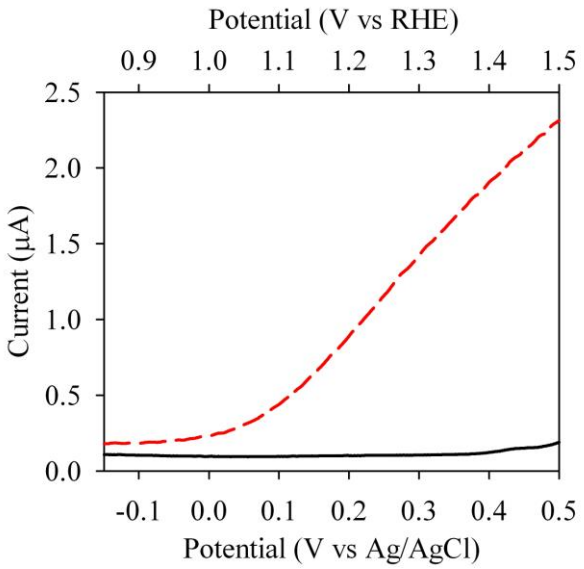

Figure S7. Linear potential sweeps of the ALD hematite electrode in the dark (black solid line) and under the illuminations of both the 400 nm pump and the white-light-continuum probe beams. Electrolyte, 1 M NaOH; Reference electrode, Ag/AgCl in 3 M NaCl; and Scanning rate, 50 mV/s.

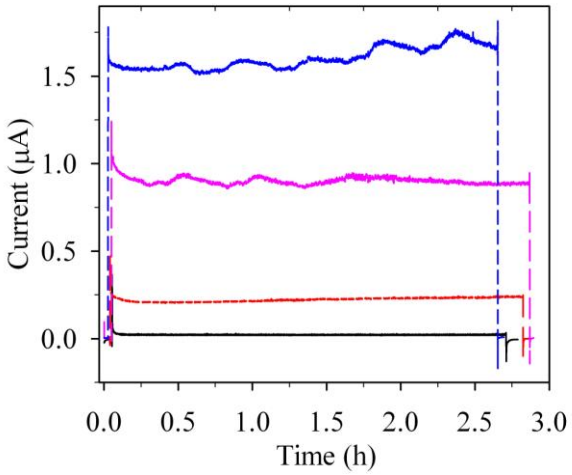

Figure S8. Current-time profiles of the ALD hematite electrode under the illumination of both the 400 nm pump and the white-light-continuum probe beams at different biases: 0.90 (black), 1.10 (red), 1.26 (pink) and 1.43 V (blue, vs RHE). The vertical lines indicate when the laser beams were unblocked (near t = 0) and blocked (after t = 2.5 h).

9. FTIR Spectra

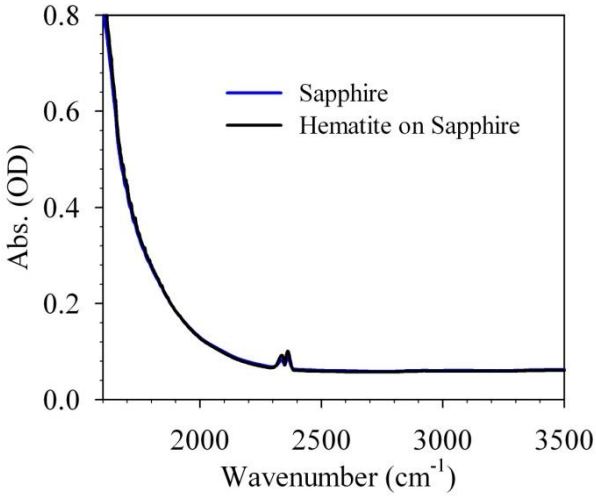

Figure S9. FTIR spectra of the sapphire substrate (blue) and 30 nm hematite ALD thin film on sapphire (black). The ground-state hematite shows no detectable IR absorption in this mid-IR window.

10. Fitting Parameters for Kinetic Traces

Table S1. Fitting parameters for kinetic traces shown in Figure 4. The kinetic traces were fitted to multi-exponential decay functions with amplitudes and time constants of (a_i, τ_i). τ_{ave} is the amplitude weighted average time constant, $\Sigma(a_i \times \tau_i) / \Sigma a_i$ (i=1-6).

	Rise time fs	τ_1, ps (a_1, %)	τ_2, ps (a_2, %)	τ_3, ps (a_3, %)	τ_4, ns (a_4, %)	τ_5, ns (a_5, %)	τ_6, ns (a_6, %)	τ_7, µs (a_7, %)	τ_{ave}
570 nm	90 ± 20	0.5 ± 0.1 (55)	135 ± 13 (10)	1150 ± 123 (17)	8 ± 1.5 (12)	67 ± 14 (4.5)	640 ± 54 (1.8)	>> 10 (0.4)	16 ± 1.8 ns
675 nm	90 ± 20	0.2 ± 0.2 (73)	1.9 ± 0.2 (15)	43 ± 8 (6.3)	1.7 ± 0.3 (3.9)	401 ± 41 (1.2)	644 ± 80 (0.2)	>>10 (0.3)	2.6 ± 0.6 ns
2000 cm^{-1}	80 ± 20	0.20 ± 0.06 (94)	1.8 ± 0.6 (4.6)	35 ± 3 (1.4)	--	--	--	--	0.7 ± 0.1 ps

11. Reference

(1) Shin, Y. K.; Brunschwig, B. S.; Creutz, C.; Sutin, N. *J Phys Chem-Us* **1996**, *100*, 8157.

(2) Lin, Y. J.; Zhou, S.; Sheehan, S. W.; Wang, D. W. *J Am Chem Soc* **2011**, *133*, 2398.

(3) Spray, R. L.; Choi, K. S. *Chem Mater* **2009**, *21*, 3701.

(4) Spray, R. L. M., J. K.; Choi, Y.-S. *J. Phys. Chem. C* **2011**, *115*, 3497.

(5) He, Y. T.; Wan, J. M.; Tokunaga, T. *J Nanopart Res* **2008**, *10*, 321.

(6) Glasscock, J. A.; Barnes, P. R. F.; Plumb, I. C.; Bendavid, A.; Martin, P. J. *Thin Solid Films* **2008**, *516*, 1716.

(7) Kerker, M.; Scheiner, P.; Cooke, D. D.; Kratohvil, J. P. *Abstr Pap Am Chem S* **1979**, 44.